Available online at www.sciencedirect.com
ScienceDirect
Journal of Sound and Vibration 319 (2009) 163–181
JOURNAL OF SOUND AND VIBRATION
www.elsevier.com/locate/jsvi

An acceleration residual generation approach for structural damage identification

Feng Gao[a], Yong Lu[b,*]

[a]School of Civil and Environmental Engineering, Nanyang Technological University, Nanyang Avenue, Singapore 639798, Singapore
[b]Institute for Infrastructure and Environment, School of Engineering and Electronics, University of Edinburgh, The King's Buildings, Edinburgh EH9 3JL, UK

Received 25 July 2007; received in revised form 20 May 2008; accepted 7 June 2008
Handling Editor: A.V. Metrikine
Available online 6 August 2008

Abstract

A residual generation approach using time-domain acceleration signals is presented for the detection of occurrence and location of damage in a structural system. An explicit damage indicator is also incorporated in the acceleration-based residual generators for the estimation of the severity of damage in individual elements. The formulation of the acceleration residual generators for damage detection extends from a previous work in the literature where displacements and velocities were considered. The basic idea of the damage residual generation is to transform the state–space description of a dynamic system with structural (stiffness) changes in different elements into multi-failure events. Consequently, the damage detection becomes effectively a disturbances decoupling problem (DDP) in control terminology, so that a geometric technique can be employed to design residual generators for individual components of the structure. By analyzing the residual error signal with an error model, the damage severity of a component can be established. Numerical and experimental examples are given to illustrate the implementation and the effectiveness of the approach.

1. Introduction

Time-domain methods for structural damage identification are seemingly attractive for real-time applications simply because they do not involve domain change. Typical time-domain damage diagnosis methods follow a similar routine. A mathematical model is set up in terms of a selected structural dynamic response parameter, e.g., the restoring force, acceleration, displacement, or velocity. The reference (baseline) model parameters are estimated from the signals measured from the undamaged state of the structure. The baseline model is then applied on the signals measured from an unknown state of the same structure. By analyzing the residual errors between the projected and actually measured signals, an indicative feature is extracted which is then interpreted for the diagnosis of the damage. Masri et al. [1] employed the neural network technique to set up a black box that predicts the restoring force, and the root mean square error ratio

*Corresponding author. Tel.: +44 1316519052; fax: +44 1316506781.
E-mail address: yong.lu@ed.ac.uk (Y. Lu).

0022-460X/$ - see front matter © 2008 Elsevier Ltd. All rights reserved.
doi:10.1016/j.jsv.2008.06.014

was used as the damage feature. Sohn and Farrar [2] proposed a two-step AR–ARX (auto-regressive–auto-regressive with eXogenous) model to predict the time series and subsequently used the standard deviation (S.D.) ratio of the residual error to indicate the damage. Lu and Gao [3] used an ARX model to detect structural damages with acceleration signals. A Kalman-filter based procedure was also adopted to process noisy signals to enhance the time-domain feature extraction [4].

Most of the time-domain methods, however, face a common problem that the general statistical features extracted directly from the time-domain signals are related vaguely to the overall state of the structure, and there is a lack of explicit link between the a damage feature and the damage in individual elements. This difficulty lies in the fact that the time-domain signals are usually measured from a selected number of degree of freedom (dof). Without implementing a pertinent decomposition procedure, it is not possible to separate the condition of each connecting member from the information extracted from a common dof.

To overcome the above difficulty in using the time-domain methods, it is necessary to find a more explicit way to link the damage of each individual component to a certain damage feature. Ma et al. [5] proposed a time-domain method for detecting structural changes in individual components. Using a linear lumped mass shear frame model, it was demonstrated that the state–space description of the dynamic equation of the system involving stiffness changes (representing damage) can be arranged into a form analogous to the extension of fundamental problem of residual generation (EFPRG) to multiple failure events. The EFPRG was originally introduced in the control literature as a disturbances decoupling problem (DDP), and a procedure for the design of the residual generators was also developed using the geometric approach [6,7]. In the study by Ma et al. [5], this technique was employed to design separate generators for individual elements in the structural dynamic system. By processing the measured signals, each generator could detect the failure of individual components separately. The results showed that the method was applicable for both stationary (white noise) and non-stationary (El Centro earthquake) ground excitations. In a more recent study by Ma et al. [8], the methodology was presented in the context of subspace decomposition such that damage in each element or location is associated with an independent single-degree-of-freedom (sdof) system. However, in both studies mentioned above, the measured time series are assumed to be displacement or velocity vectors. Moreover, the severity of damage was estimated with a traditional system identification method that requires an iteration procedure [8].

Considering the fact that acceleration measurement is commonly used in structural health monitoring applications, this paper presents a formulation that enables the construction of residual generators for damage in individual elements/locations using acceleration signals. Unlike the models based on displacement or velocity, in the acceleration-based model the two system matrices are both affected when damage is introduced in terms of a stiffness change. Hence, the failure modes and disturbances cannot be figured out in a straightforward manner and a re-formulation of the problem is required, as described in Section 3. The implementation of the proposed approach is illustrated through two representative numerical examples and a laboratory experimental case.

2. Overview of the formulation of EFPRG to multiple failure events

Generally speaking, the EFPRG is a DDP, which was originally developed in the control field [6,7]. In this section, the EFPRG is briefly introduced and the solution known as the residual generator technique is also described.

The formulation of the EFPRG follows a description of a nominal linear time invariant (LTI) system in the form:

$$\dot{\mathbf{x}}(t) = \mathbf{A}\mathbf{x}(t) + \mathbf{B}\mathbf{u}(t) + \sum_{i=1}^{k} \mathbf{P}_i m_i(t)$$

$$\mathbf{y}(t) = \mathbf{C}\mathbf{x}(t) \tag{1}$$

The above equation describes a *system* ($\mathbf{C}$, $\mathbf{A}$, $\mathbf{B}$). The nominal input $\mathbf{u}(t)$ and the output $\mathbf{y}(t)$ are assumed to be known. The signals $m_i(t)$ are arbitrary and unknown functions of time, representing the ith actuator failure mode. The *map* $\mathbf{P}_i$: $m_i \rightarrow \mathbf{X}$ is referred to as the ith actuator failure signature. The range of $\mathbf{P}_i$ is regarded as the

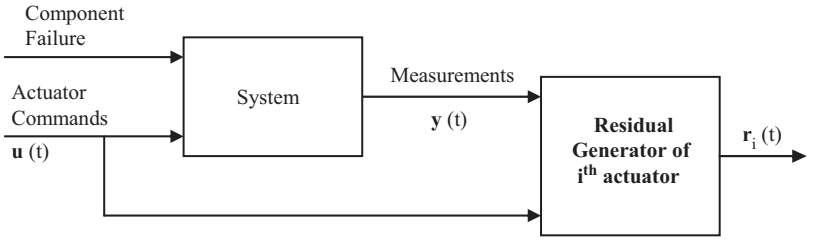

Fig. 1. Block diagram of a residual generator.

disturbance from the ith actuator. If there is no disturbance from the ith actuator, the signal $m_i(t)$ is essentially a zero signal.

The EFPRG may be solved by designing k residual generators, and a standard procedure for such purpose was developed by Massoumnia et al. [7]. It is desired that a nonzero $m_i(t)$ should affect the residual signal of the ith residual generator, $r_i(t)$, and only this generator. At the same time, other nonzero $m_j(t)$ ($j \neq i$) should not affect $r_i(t)$ of this residual generator. The process of one such generator is depicted with a block diagram in Fig. 1.

According to Ref. [7], such residual generator has a general form for a realizable LTI processor that takes the observables $\mathbf{y}(t)$ and $\mathbf{u}(t)$ as inputs and generates a residual $r_i(t)$ as:

$$\begin{aligned} \dot{\mathbf{w}}(t) &= \mathbf{F}\mathbf{w}(t) - \mathbf{E}\mathbf{y}(t) + \mathbf{G}\mathbf{u}(t) \\ r_i(t) &= \mathbf{M}\mathbf{w}(t) - \mathbf{H}\mathbf{y}(t) \end{aligned} \tag{2}$$

where $\mathbf{E}$, $\mathbf{F}$, $\mathbf{G}$, $\mathbf{M}$ and $\mathbf{H}$ are coefficients.

The residual generator represented by Eq. (2) is designed for a specific actuator, so that when the particular actuator failure mode is present, a nonzero signal $m_i(t)$ can lead to a nonzero $r_i(t)$. Thus, $r_i(t)$ calculated from Eq. (2) becomes the monitor of the ith actuator.

When the system [$\mathbf{A}$, $\mathbf{B}$, $\mathbf{C}$, $\mathbf{D}$, $\mathbf{P}_i$ ($i = 1,\ldots,k$)] is provided and satisfies the solution condition (Appendix B), a geometric approach can be used to develop these monitors. According to Ref. [7], the coefficients of Eq. (2) should satisfy the following conditions:

$$\mathbf{F} = \mathbf{A}_0 + \mathbf{D}_1\mathbf{M}, \quad \text{where } \mathrm{eig}(\mathbf{F}) = \mathbf{\Lambda} \text{ with negative eigenvalue;}$$

$$\mathbf{E} = \mathbf{O}\mathbf{D}_0 + \mathbf{D}_1\mathbf{H}, \quad \mathbf{G} = \mathbf{O}\mathbf{B}, \quad \mathbf{M} = \mathbf{H}\mathbf{C}\mathbf{O}^{-r}, \quad \mathbf{H}\mathbf{C}\mathbf{P}_{j\neq i} = 0, \quad \text{and } \mathbf{H}\mathbf{C}\mathbf{P}_i \neq \mathbf{0}$$

For $\mathbf{O}$, $\mathbf{D}_0$, and $\mathbf{A}_0$, it has:

$$\mathbf{O}(\mathbf{A} + \mathbf{D}_0\mathbf{C})x(t) = \mathbf{A}_0\mathbf{O}\mathbf{x}(t), \quad \mathbf{O}\mathbf{P}_{j\neq i} = \mathbf{0}, \quad \text{and } \mathbf{O}\mathbf{P}_i \neq \mathbf{0}$$

Further information on the procedure is given in Appendix A.

Using Eqs. (1) and (2), and arranging, it follows:

$$\begin{aligned} \dot{\mathbf{w}}(t) - \mathbf{O}\dot{\mathbf{x}}(t) &= \mathbf{F}\mathbf{w}(t) - (\mathbf{O}\mathbf{D}_0 + \mathbf{D}_1\mathbf{H})\mathbf{y}(t) + \mathbf{G}\mathbf{u}(t) - \mathbf{O}\mathbf{A}\mathbf{x}(t) - \mathbf{O}\mathbf{B}\mathbf{u}(t) - \mathbf{O}\sum_{i=1}^{k}\mathbf{P}_i m_i(t) \\ &= \mathbf{F}\mathbf{w}(t) - (\mathbf{O}\mathbf{D}_0 + \mathbf{D}_1\mathbf{H})\mathbf{C}\mathbf{x}(t) + \mathbf{O}\mathbf{B}\mathbf{u}(t) - \mathbf{O}\mathbf{A}\mathbf{x}(t) - \mathbf{O}\mathbf{B}\mathbf{u}(t) - \mathbf{O}\sum_{i=1}^{k}\mathbf{P}_i m_i(t) \\ &= \mathbf{F}\mathbf{w}(t) - \mathbf{O}(\mathbf{A} + \mathbf{D}_0\mathbf{C})\mathbf{x}(t) - \mathbf{D}_1\mathbf{H}\mathbf{C}\mathbf{x}(t) - \mathbf{O}\sum_{i=1}^{k}\mathbf{P}_i m_i(t) \end{aligned} \tag{3}$$

With the aforementioned definition of the coefficients, the above equation can be rewritten as:

$$\dot{\mathbf{w}}(t) - \mathbf{O}\dot{\mathbf{x}}(t) = \mathbf{F}\mathbf{w}(t) - (\mathbf{A}_0 + \mathbf{D}_1\mathbf{M})\mathbf{O}\mathbf{x}(t) - \mathbf{O}\mathbf{P}_i m_i(t) \tag{4}$$

Defining $\mathbf{e}(t) = \mathbf{w}(t) - \mathbf{O}\mathbf{x}(t)$, the state–space model in Eq. (2) can be expressed as:

$$\begin{aligned} \dot{\mathbf{e}}(t) &= \mathbf{F}\mathbf{e}(t) - \mathbf{O}\mathbf{P}_i m_i(t) \\ r_i(t) &= \mathbf{M}\mathbf{e}(t) \end{aligned} \tag{5}$$

In Eq. (5), $\dot{\mathbf{e}}(t)$ is expressed with $m_i(t)$ as the only input. It follows that the system relating $m_i(t)$ to $\mathbf{e}(t)$ is *input observable* (the disturbance signal of $m_i(t)$ can effect signal $\mathbf{e}(t)$); and obviously other disturbances $m_{j\neq i}(t)$ are *unobservable* (the disturbance of $m_{j\neq i}(t)$ will not lead to disturbance of signal $\mathbf{e}(t)$). Hence, $r_i(t)$ is not affected by signals $m_{j\neq i}(t)$. Only when $m_i(t)$ exhibits failure of the ith actuator, $r_i(t)$ will become effectively nonzero. Thus, $r_i(t)$ satisfies the requirement of the solution as an indicator of the ith actuator.

3. Problem formulation for acceleration-based damage diagnosis

For a structural dynamic system, the equation of motion can be expressed as:

$$\mathbf{M}_0\ddot{\xi}(t) + \mathbf{C}_0\dot{\xi}(t) + \mathbf{K}_0\xi(t) = \mathbf{L}_0\mathbf{u}(t) \tag{6}$$

where $\mathbf{u}(t)$ is the input vector; $\mathbf{M}_0$, $\mathbf{C}_0$, $\mathbf{K}_0$ are mass, damping, and stiffness matrices, respectively; and $\mathbf{L}_0$ is a load matrix.

The above dynamic equation can also be expressed in a state–space form for a linear system:

$$\begin{aligned} \dot{\mathbf{x}}(t) &= \mathbf{A}\mathbf{x}(t) + \mathbf{B}\mathbf{u}(t) \\ \mathbf{y}(t) &= \mathbf{C}\mathbf{x}(t) + \mathbf{L}\mathbf{u}(t) \end{aligned} \tag{7}$$

where $\mathbf{x}(t)$ is the state vector, $\mathbf{u}(t)$ denotes the excitation and $\mathbf{y}(t)$ is the structural response. When $\mathbf{y}(t)$ and $\mathbf{u}(t)$ are confined as accelerations, the coefficient matrices in Eq. (7) can be determined [9] as:

$$\mathbf{A} = \begin{bmatrix} -\mathbf{J} & \mathbf{I} \\ -\mathbf{K} & 0 \end{bmatrix}, \quad \mathbf{B} = \begin{bmatrix} -\mathbf{J}\mathbf{L} \\ -\mathbf{K}\mathbf{L} \end{bmatrix}, \quad \mathbf{C} = \begin{bmatrix} \mathbf{I} & 0 \end{bmatrix} \tag{8}$$

where $\mathbf{K}$, $\mathbf{J}$, $\mathbf{L}$ are mass normalized stiffness, damping and load matrices, respectively, $\mathbf{K} = \mathbf{M}_0^{-1}\mathbf{K}_0$, $\mathbf{J} = \mathbf{M}_0^{-1}\mathbf{C}_0$, and $\mathbf{L} = \mathbf{M}_0^{-1}\mathbf{L}_0$.

If the effect of damage in different components of the structure can be transformed as failure of different actuators, then the solution of EFPRG can be applied to identify the damage in individual components of the structure. Consider the structural changes in the form of stiffness reduction only, and assume the damping matrix $\mathbf{J}$ and load matrix $\mathbf{L}$ remain unchanged. Hence, defining $\mathbf{y}^t(t) = \mathbf{y}(t) - \mathbf{L}\mathbf{u}(t)$ as the system output, the second formula in Eq. (7) can be simplified as $\mathbf{y}^t(t) = \mathbf{C}\mathbf{x}(t)$.

When stiffness changes occur, the model parameters $\mathbf{A}$ and $\mathbf{B}$ will change in accordance with Eq. (8). Thus, the system with damage can be written as:

$$\dot{\mathbf{x}}(t) = \mathbf{A}\mathbf{x}(t) + \mathbf{B}\mathbf{u}(t) + \Delta\mathbf{A}\mathbf{x}(t) + \Delta\mathbf{B}\mathbf{u}(t), \quad \mathbf{y}^t(t) = \mathbf{C}\mathbf{x}(t) \tag{9}$$

Define $\Delta\mathbf{K}$ as the change of the stiffness matrix $\mathbf{K}$ due to damage in some components. It is possible to decompose $\Delta\mathbf{K}$ into the following form (Appendix C):

$$\Delta\mathbf{K} = \sum_{i=1}^{k} \mathbf{p}_i\mathbf{q}_i\alpha_i \tag{10}$$

where k is the number of structural components potentially with damage, α_i denotes the damage severity of the ith component, $\mathbf{p}_i$ and $\mathbf{q}_i$ are the decomposed matrices of the stiffness of the ith component in the global stiffness matrix. $\mathbf{p}_i$ and $\mathbf{q}_i$ are targeted to have as fewer as possible columns and rows, respectively.

$\Delta\mathbf{A}$ and $\Delta\mathbf{B}$ can then be written as:

$$\Delta\mathbf{A} = \begin{bmatrix} 0 & 0 \\ -\Delta\mathbf{K} & 0 \end{bmatrix} = -\sum_{i=1}^{k} \begin{bmatrix} \mathbf{0} \\ \mathbf{p}_i \end{bmatrix} \begin{bmatrix} \mathbf{q}_i, & \mathbf{0} \end{bmatrix} \alpha_i$$

$$\Delta\mathbf{B} = \begin{bmatrix} \mathbf{0} \\ -\Delta\mathbf{K}\mathbf{L} \end{bmatrix} = -\sum_{i=1}^{k} \begin{bmatrix} \mathbf{0} \\ \mathbf{p}_i \end{bmatrix} \mathbf{q}_i \mathbf{L} \alpha_i \tag{11}$$

Subsequently,

$$\begin{aligned} \Delta\mathbf{A}\mathbf{x}(t) + \Delta\mathbf{B}\mathbf{u}(t) &= -\sum_{i=1}^{k} \begin{bmatrix} \mathbf{0} \\ \mathbf{p}_i \end{bmatrix} [\mathbf{q}_i, \quad \mathbf{0}] \alpha_i \mathbf{x}(t) - \sum_{i=1}^{k} \begin{bmatrix} \mathbf{0} \\ \mathbf{p}_i \end{bmatrix} \mathbf{q}_i \mathbf{L} \alpha_i \mathbf{u}(t) \\ &= -\sum_{i=1}^{k} \begin{bmatrix} \mathbf{0} \\ \mathbf{p}_i \end{bmatrix} \alpha_i ([\mathbf{q}_i, \quad \mathbf{0}] \mathbf{x}(t) + \mathbf{q}_i \mathbf{L}\mathbf{u}(t)) \\ &= \sum_{i=1}^{k} \mathbf{P}_i m_i(t) \end{aligned} \tag{12}$$

Here the failure signatures are: $\mathbf{P}_i = [\mathbf{0} \quad \mathbf{p}_i]^{\mathrm{T}}$ for each component, and the disturbance $m_i(t)$ has the form:

$$m_i(t) = -\alpha_i(\mathbf{q}_i \cdot [\mathbf{I}, \quad \mathbf{0}]\mathbf{x}(t) + \mathbf{q}_i \mathbf{L}\mathbf{u}(t)) = -\alpha_i \mathbf{q}_i (\mathbf{C}\mathbf{x}(t) + \mathbf{L}\mathbf{u}(t)) = -\alpha_i \mathbf{q}_i \mathbf{y}(t) \tag{13}$$

Although this definition of $m_i(t)$ is not necessary for the implementation of EFPRG, it facilitates the estimation of the damage severity, as will be described in Section 4.

Substitution of Eq. (12) in Eq. (9) yields the model with multi-failures events as:

$$\begin{aligned} \dot{\mathbf{x}}(t) &= \mathbf{A}\mathbf{x}(t) + \mathbf{B}\mathbf{u}(t) + \sum_{i=1}^{k} \mathbf{P}_i m_i(t) \\ \mathbf{y}^f(t) &= \mathbf{C}\mathbf{x}(t) \end{aligned} \tag{14}$$

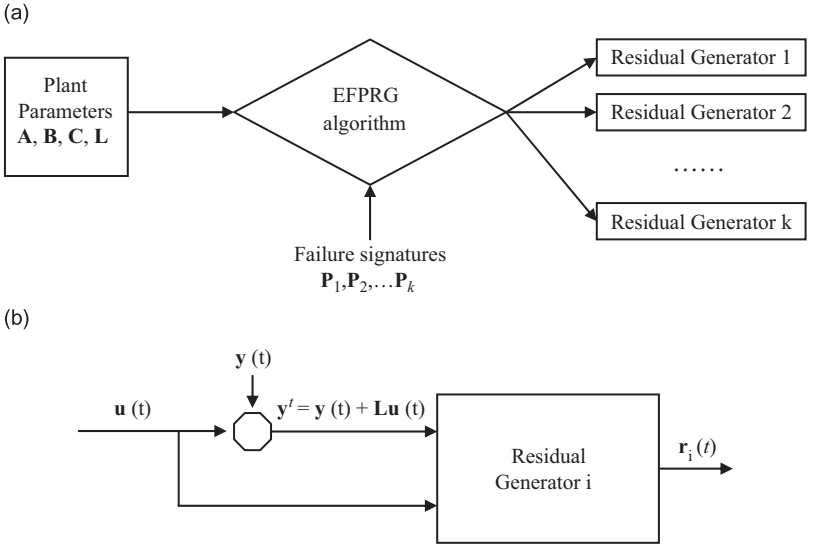

Fig. 2. Standard procedure of design of residual generators and residual generation: (a) block diagram for the design of residual generator and (b) block diagram for residual generation for ith component.

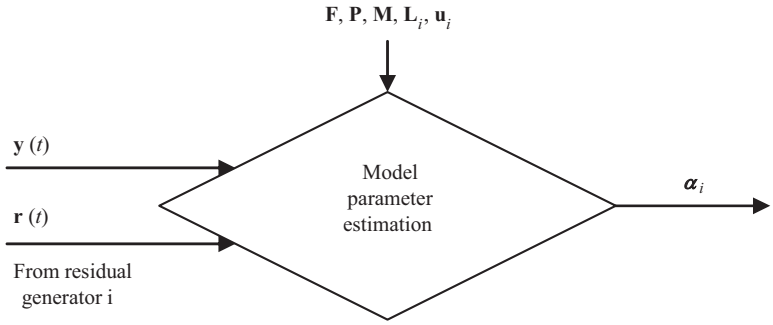

Fig. 3. Block diagram for evaluation of damage severity.

Through the above transformation, the damage in different components can be described as the actuator failure of *system* (**C**, **A**, **B**). Now the geometric approach can be used to design the residual generators of Eq. (14), which has the standard form of EFPRG as expressed in Eq. (1). The damage signature of the ith component, $\mathbf{P}_i = [\mathbf{0} \quad \mathbf{p}_i]^{\mathrm{T}}$, can be determined following the element stiffness decomposition procedure (Appendix C). The diagrams for designing the residual generators and the procedure of residual generation are shown in Fig. 2. More detailed procedure for the design of the residual generator for an individual component is given in Appendix B. Thereafter, the damage status of the ith component can be assessed by examining the level of the residual error signal $r_i(t)$ from the ith generator.

4. Evaluation of damage severity

Totally, k number of residual generators will be designed and each generator represents one particular component. As can be seen from Eqs. (10) to (12), in order for the generators to provide consistent results, the k number of generators should cover all components that may be subject to damage and hence contribute in the change of the global stiffness ΔK. Then the monitoring results should not be affected by the choice of k. Subsequently, it becomes possible to evaluate the damage severity of individual components by further examining the residual error $r_i(t)$, as explained in what follows.

Using the definition of $m_i(t)$ in Eq. (13), from Eq. (5) we get:

$$\begin{aligned} \dot{\mathbf{e}}(t) &= \mathbf{F}\mathbf{e}(t) + \alpha_i \mathbf{O}_i \mathbf{P}_i \mathbf{q}_i \mathbf{y}(t) \\ r_i(t) &= \mathbf{M}\mathbf{e}(t) \end{aligned} \tag{15}$$

With the generator parameters obtained as described in Appendix B, and $\mathbf{y}(t)$, $\mathbf{u}(t)$ available from the measurement, $r_i(t)$ can be obtained from the ith generator by Eq. (2). On determining the decomposed stiffness component $\mathbf{q}_i$ as described in Appendix C, the damage severity factor α_i becomes the only unknown parameter in Eq. (15) and hence can be easily evaluated. The block diagram for the evaluation of the damage severity factor α_i is shown in Fig. 3.

5. Numerical examples

In this section, the proposed approach is applied on two numerical examples, namely a three-storey lumped mass frame and a truss, to illustrate its implementation and effectiveness in the structural damage diagnosis. It should be noted that the present method requires all dof in the representative dynamic model of the structure to be measurable. Considering the practical difficulty in the measurement of rotational signals, these numerical examples do not involve joint rotations. Nevertheless, in principle, the method is applicable for structures with joint rotations so long as the rotational response signals are available.

The three-storey lumped mass system is identical to the example used by Ma et al. [5]; however, herein acceleration signals are used instead of displacements and the damage severity is also calculated. The truss

system is employed to further demonstrate the applicability of the method in a more complex situation with multiple members connecting at a common joint.

In these examples, the mass, stiffness, and damping of the undamaged system are pre-selected. The time series of the acceleration measurements under various damage scenarios are simulated by a structural dynamic response analysis. These signals are used as the available measurements for the damage diagnosis. The effects of the model accuracy and the measurement noise on the performance of the method will be discussed with a laboratory experimental case in Section 6.

In implementing the models for the generators and the damage severity, the continuous formulation described in the previous sections are transformed into the discrete models by a standard zero-order-hold discretization. For the state–space model, it has [11]:

$$\begin{aligned}\mathbf{x}(k+1) &= \mathbf{A}_D\mathbf{x}(k) + \mathbf{B}_D\mathbf{u}(k)\\ \mathbf{y}(k) &= \mathbf{C}\mathbf{x}(k)\end{aligned} \tag{16}$$

where

$$\mathbf{A}_D = \sum_{j=0}^{\infty} \frac{(\mathbf{A}\Delta t)^j}{j!}, \quad \text{and} \quad \mathbf{B}_D = \mathbf{A}^{-1}(\mathbf{A}_D - \mathbf{I})\mathbf{B}$$

5.1. Three-story lumped mass shear frame

The three-story lumped mass shear frame, shown in Fig. 4, is assumed to have uniform properties in all storeys, with mass $M_i = 1000\,\text{kg}$, stiffness $K_i = 980\,\text{kN/m}$, and damping coefficient $C_i = 1.407\,\text{kN-s/m}$. The natural frequencies of the frame are evaluated to be 2.22, 6.21 and 8.97 Hz, respectively. The damage is represented by stiffness changes. The simulated damage scenarios include single- and multiple-damage scenarios with different damage severity. A broad-band white noise acceleration with a standard deviation of $1\,\text{m/s}^2$ is used to excite the structure at the base. The measurements include the accelerations at the three-storey levels.

Applying the procedure described in Appendix C, the failure signatures for the three-storey stiffness factors are found to be:

$$\mathbf{P}_1 = \begin{bmatrix}0, & 0, & 0, & 0, & 0, & 1\end{bmatrix}^{\mathrm{T}}$$

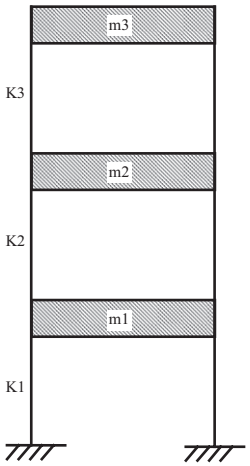

Fig. 4. A three-storey lumped mass frame model.

$$\mathbf{P}_2 = \begin{bmatrix} 0, & 0, & 0, & 0, & -1, & 1 \end{bmatrix}^{\mathrm{T}}$$

$$\mathbf{P}_3 = \begin{bmatrix} 0, & 0, & 0, & -1, & 1, & 0 \end{bmatrix}^{\mathrm{T}}$$

Referring to Appendix B, in the present case $k_i = 1$ for actuators 1, 2 and 3, and $l = 3$, $v = 3$, $n = 6$, the generic solvability conditions $v \leqslant n$ and $v - \min\{k_i, i \in k\} < l$ are satisfied. Then three monitors, designated as No. 1, 2, and 3, can be designed to monitor the stiffness coefficients K_1, K_2, and K_3, respectively. The design of one residual generator, $\mathbf{r}_2(t)$, is described in more detail as an example in what follows.

First, the subspace W_2^* of (**C, A**)-*invariant* is given by the following ***CAISA*** ((**C**, **A**)-***I**nvariant **S**ubspace **A**lgorithm*) (Appendix A):

$$\mathsf{W}_2^* = \mathsf{P}_1 \oplus \mathsf{P}_3 \oplus \mathbf{A}\mathsf{P}_1 \oplus \mathbf{A}\mathsf{P}_3$$

Thus, the insertion map $\mathbf{W}_2 : \mathsf{W}_2^* \to \mathsf{X}$ is $\mathbf{W}_2 = [\mathbf{P}_1, \mathbf{P}_3, \mathbf{AP}_1, \mathbf{AP}_3]$.

S_2^* as (**C**, **A**)-*u.o.s.* (**UnO**bservability **S**ubspace) is obtained by the following ***UOSA*** (***UnO**bservability **S**ubspace **A**lgorithm*, see Appendices A and B):

$$\mathsf{S}_2^* + Ker\mathbf{C} = \mathsf{W}_2^* + Ker\mathbf{C}$$

- *Step* 1: $\mathbf{D}_0 = -\mathbf{A}^2\begin{bmatrix}\mathbf{P}_1, & \mathbf{P}_3\end{bmatrix}\left(\mathbf{CA}\begin{bmatrix}\mathbf{P}_1, & \mathbf{P}_3\end{bmatrix}\right)^{-l}$, hence

$$\mathbf{D}_0 = \begin{bmatrix} 1.4 & 0 & 0 \\ -1.4 & 0 & 0 \\ 0 & 0 & 1.4 \\ 1960 & 0 & 0 \\ -2940 & 0 & -980 \\ 980 & 0 & 1960 \end{bmatrix}$$

- *Step* 2: Find **O** from $[\mathbf{P}_1, \mathbf{P}_2, \mathbf{P}_3, \mathbf{AP}_1, \mathbf{AP}_2, \mathbf{AP}_3]^{-1}$ by its second row and fifth row as:

$$\mathbf{O} = \begin{bmatrix} 1 & 1 & 0 & 0 & 0 & 0 \\ 0 & 0 & 0 & 1 & 1 & 0 \end{bmatrix}$$

Let $\mathbf{A}_0 = \mathbf{A} + \mathbf{D}_0\mathbf{C} : \mathsf{X}/\mathsf{S}_2^*$, $\mathbf{A}_0$ is the map induced on the factor space $\mathsf{X}/\mathsf{S}_2^*$:

$$\mathbf{A}_0 = \begin{bmatrix} 1.407 & 1 \\ -980 & 0 \end{bmatrix}$$

- *Step* 3: **H** can be calculated by

$$\mathbf{H} = \mathbf{I} - \mathbf{C}\begin{bmatrix}\mathbf{P}_1, & \mathbf{P}_3\end{bmatrix}\left(\mathbf{CA}\begin{bmatrix}\mathbf{P}_1, & \mathbf{P}_3\end{bmatrix}\right)^{-l}, \quad \mathbf{H} = \begin{bmatrix} 0 & 0 & 0 \\ 1 & 1 & 0 \\ 0 & 0 & 0 \end{bmatrix}$$

- *Step* 4: Solve for **M** from $\mathbf{MO} = \mathbf{HC}$

$$\mathbf{M} = \begin{bmatrix} 0 & 0 \\ 1 & 0 \\ 0 & 0 \end{bmatrix}$$

- *Step* 5: Let $\mathrm{eig}(\mathbf{F}) = [-1, 0; 0, -1\ ]$ that satisfies the condition of self-conjugate with negative eigenvalue; then **F** satisfing $\mathbf{F} = \mathbf{A}_0 + \mathbf{D}_1\mathbf{M}$ can be found as:

$$\mathbf{F} = \begin{bmatrix} 2 & 1 \\ -1 & 0 \end{bmatrix}$$

and hence

$$\mathbf{D}_1 = \begin{bmatrix} 0 & -0.593 & 0 \\ 0 & 979 & 0 \end{bmatrix}$$

- *Step* 6: With $\mathbf{O}^{-r}$ denoting a right inverse of $\mathbf{O}$, calculate $\mathbf{D} = \mathbf{D}_0 + \mathbf{O}^{-r}\mathbf{D}_1\mathbf{H}$, $\mathbf{E} = \mathbf{OD}$, $\mathbf{G} = \mathbf{OB}$:

$$\mathbf{D} = \begin{bmatrix} 0.8 & -0.6 & 0 \\ -1.4 & 0 & 0 \\ 0 & 0 & 1.4 \\ 2939 & 979 & 0 \\ -2940 & 0 & -980 \\ 980 & 0 & 1960 \end{bmatrix}$$

$$\mathbf{E} = \begin{bmatrix} 0.593 & -0.593 & 0 \\ -1 & 979 & -980 \end{bmatrix}$$

$$\mathbf{G} = \begin{bmatrix} -2.8140 \\ 0 \end{bmatrix}$$

Then the generator of $\mathbf{r}_2(t)$ that takes the observables $\mathbf{y}(t)$ and $\mathbf{u}(t)$ as inputs is completely established following Eq. (2) as:

$$\dot{\mathbf{w}}(t) = \mathbf{F}\mathbf{w}(t) - \mathbf{E}\mathbf{y}(t) + \mathbf{G}\mathbf{u}(t), \quad r_2(t) = \mathbf{M}\mathbf{w}(t) - \mathbf{H}\mathbf{y}(t)$$

Similarly, the generator $r_1(t)$ and $r_3(t)$ are designed. In order to keep comparable magnitudes of all residual signals, $\mathrm{eig}(\mathbf{F}) = [-1, 0; 0, -1]$ is adopted for each generator.

Figs. 5 and 6 show the output of the residual generators for different damage scenarios. Each figure includes the signals from three residual generators for a particular damage scenario. When a residual signal from a generator shows apparent nonzero signal, it indicates the occurrence of damage on the structure at the component represented by the corresponding generator. On the other hand, if a residual signal is close to zero, no change takes place at the corresponding component. From the results shown in Figs. 5 and 6, the various damage scenarios can be clearly determined.

With the residual signal generated, the damage severity can be calculated following the block diagram shown in Fig. 3. The values of α_i for the stiffness in these storeys are listed in Table 1. It can be seen that the α_i values reflect quite accurately the actual damage severity in terms of the percentage reduction of the storey stiffness.

5.2. Truss system

The truss is depicted in Fig. 7. Since multiple members are connected at certain common joints, it would be difficult to distinguish changes in individual members by analyzing the signals measured at these joints following a general time-domain method. However, using the residual generator technique it becomes possible to determine the damage status of each member.

In this example truss, each member is 0.5 m long, and all the members are made by aluminum pipe of circular section with an outer radius of 20 mm and a wall thickness of 2 mm. The modulus of elasticity of the material is $7.0 \times 10^7\,\mathrm{KN/m^2}$. Joints J1, J2 and J3 are allocated an equal lumped mass of 50 kg. The damping ratio is assumed to be 0.5% for all modes. The truss is excited at J1 with a vertical dynamic force of a broad-band white noise with a standard deviation of 50 N. The accelerations at the three free joints (6-dofs) shown in Fig. 7 are taken as the measurements.

Six residual generators are designed, one for each member of the truss. Two damage scenarios are chosen to demonstrate the results, one with a stiffness reduction of 20% in member 2, another with a stiffness reduction of 20% in both members 2 and 4.

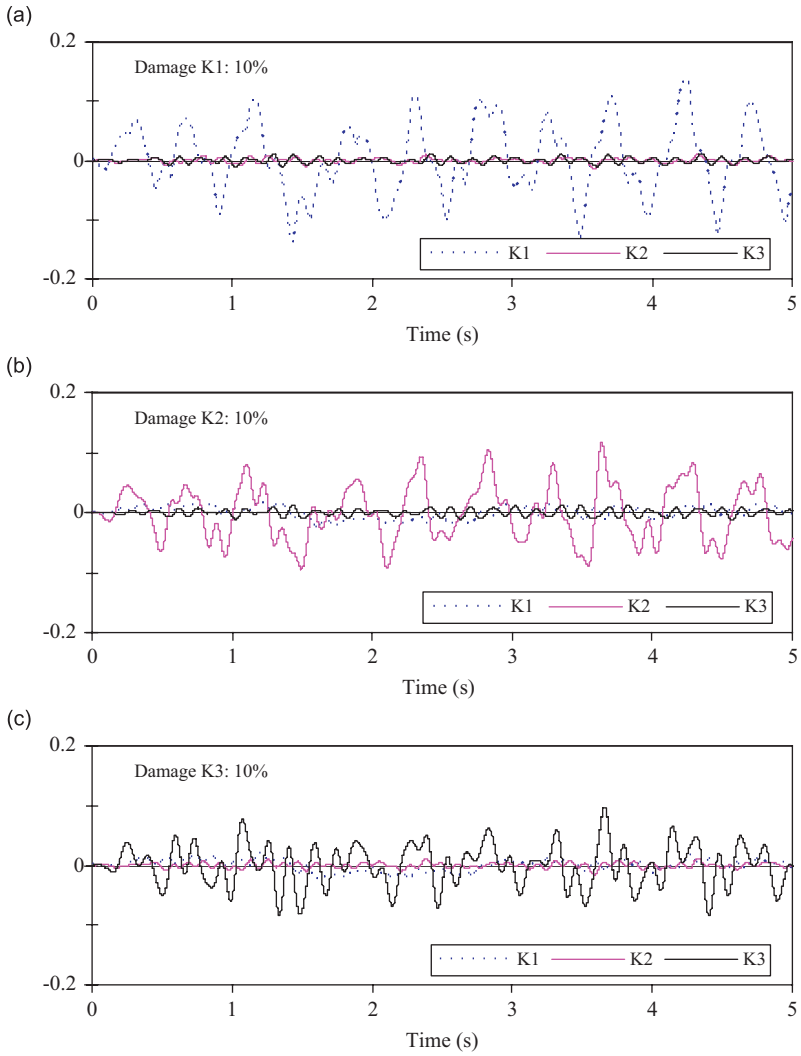

Fig. 5. Acceleration residual error signals for single-damage scenarios: (a) reduction of K1 by 10%, (b) reduction of K2 by 10%, and (c) reduction of K3 by 10%.

The output from generators for K2 and K4 are plotted in Fig. 8. The signals from other generators are not shown because they are essentially zero for these cases. From the figure, the damaged members can be easily detected by the large residual error. The values of α_i for the three truss members are listed in Table 2. It can be observed that the percentage stiffness changes are fairly well identified.

6. Experimental study

In this section, the proposed method is applied on an experimental case to verify its workability and effectiveness under an actual structural and measurement condition. For illustrative purpose with an emphasis on the real measurements, a relatively simple model structure is chosen.

For the design of the residual generators, a basic structural (finite element) model needs to be established first for the general description of the actual structural system in question. Although it is desirable that the model describes closely the actual structure, the absolute accuracy of the model does not necessarily cast a problem as far as the relative change of the structural (stiffness) condition is concerned. The accuracy of the FE model in representing the actual structure would be reflected in the absolute residual errors. Once a baseline residual

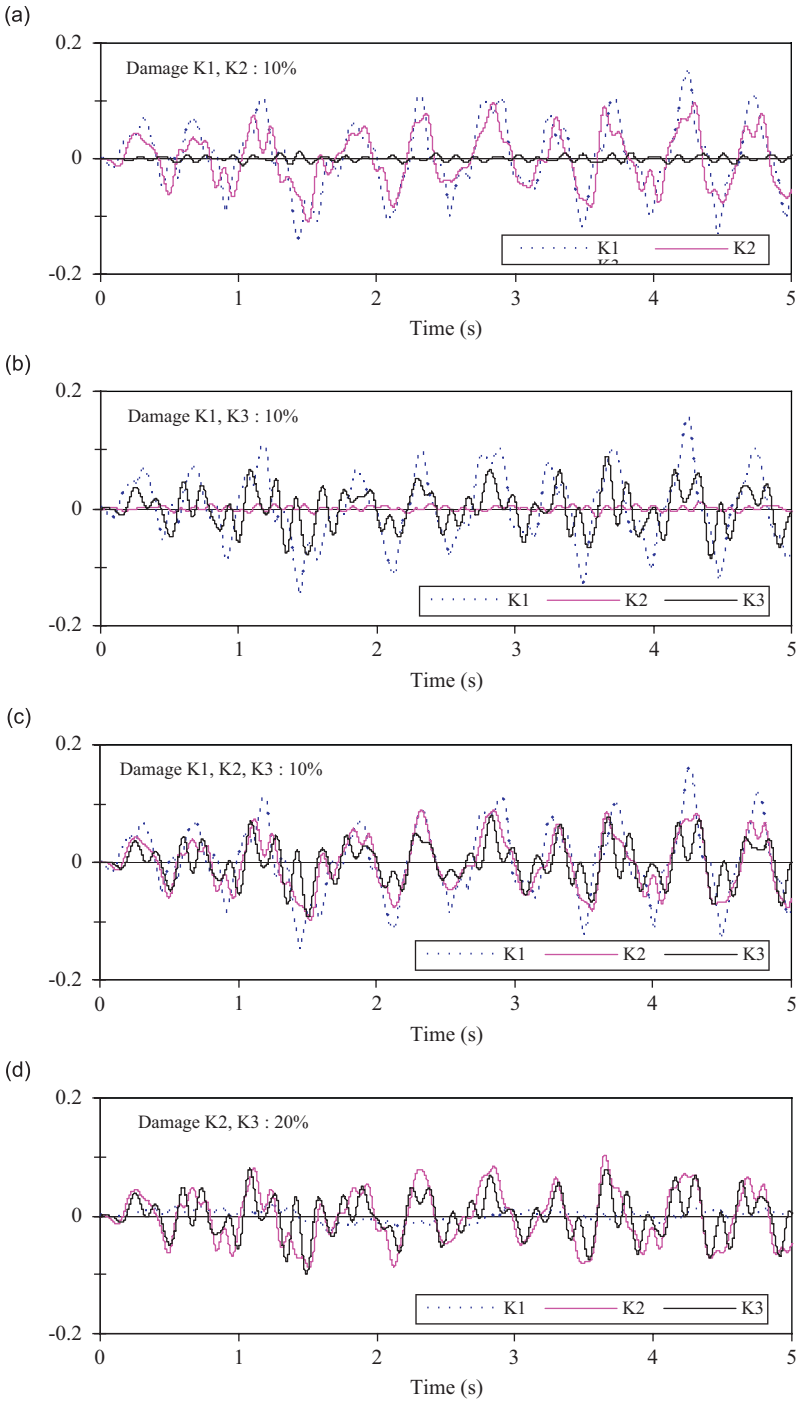

Fig. 6. Acceleration residual error signals for multiple-damage scenarios: (a) reduction of K1 and K2 by 10% each; (b) reduction of K1 and K3 by 10% each; (c) reduction of K1, K2 and K3 by 10% each; and (d) reduction of K2 and K3 by 20% each.

error is established for a reference state of the structure, the future monitoring can be based on the relative deviation of the residual error signals with respect to the baseline error. From this point of view, the accuracy of the finite element model should not affect sensibly the monitoring effect, as will be shown later in this experimental example.

Table 1
Results of damage severity (α values) for the shear frame example

Damage scenarios	α_1 for K1	α_2 for K2	α_3 for K3
No damage	0.15%	−0.04%	−0.02%
K1 10% damage	10.12%	−0.06%	−0.02%
K2 10% damage	0.15%	9.97%	−0.02%
K3 10% damage	0.14%	−0.03%	9.98%
K1 and K2 10% damage	10.12%	9.97%	−0.02%
K1 and K3 10% damage	10.12%	−0.04%	9.98%
K2 and K3 10% damage	0.14%	9.97%	9.98%
K2 and K3 20% damage	0.16%	19.97%	19.98%
K1, K2, and K3 10% damage	10.12%	9.97%	9.98%

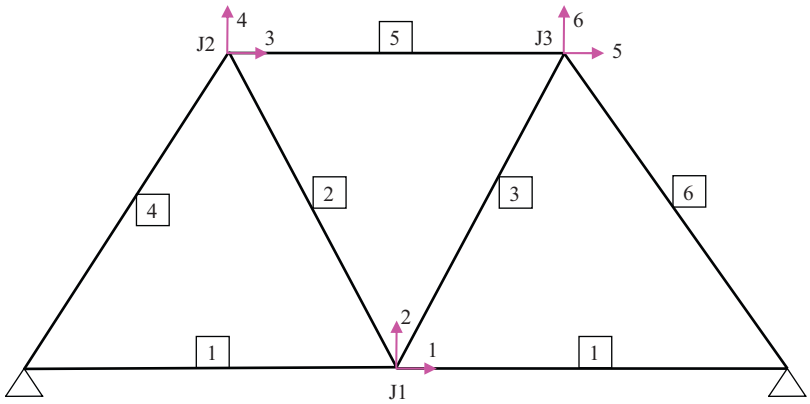

Fig. 7. Example truss showing component and dof numbers.

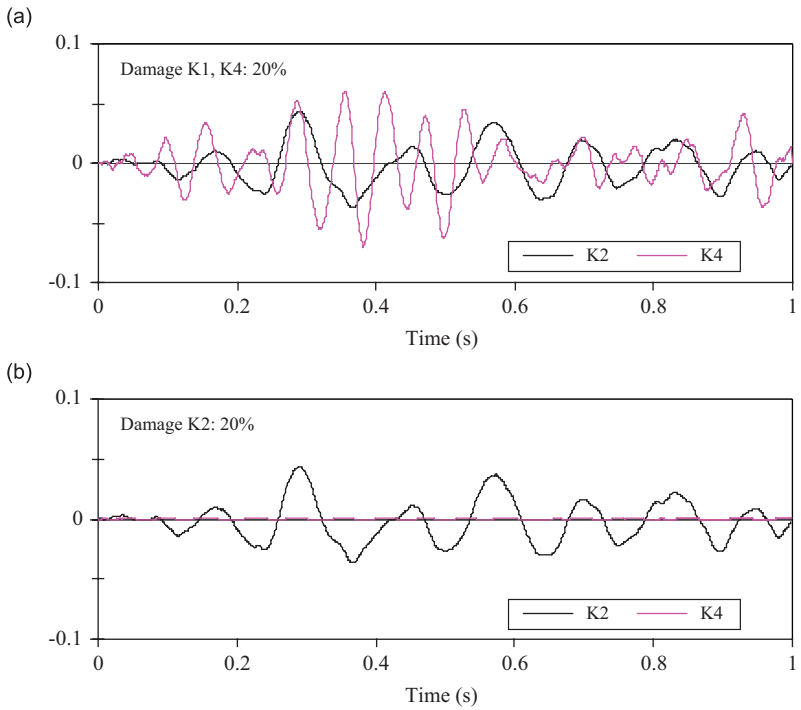

Fig. 8. Acceleration residual error signals from generators K2 and K4: (a) damage 20% on both K2 and K4 and (b) damage 20% on K2.

Table 2
Results for damage severity (α values) for the truss example

Damage scenarios	α_2 for K2	α_4 for K4
K2 and K4 20% damage	21.73%	20.54%
K2 20% damage	20.46%	0.50%

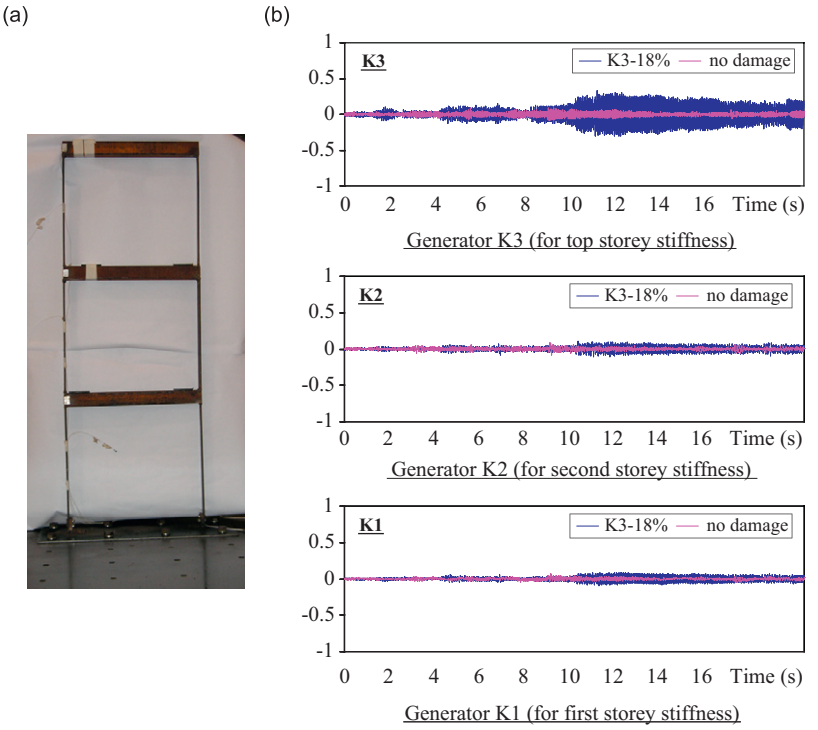

Fig. 9. Laboratory test frame and residual error signals generated from the three monitors: (a) test frame and (b) acceleration residual error signals.

The test structure is a model steel frame, shown in Fig. 9. The beams are purposely made stiff with a hollow box section of 50 mm × 50 mm × 3 mm. The columns are to be monitored and they are made of flat steel bars with a cross-section of 50 mm × 6 mm. The weaker axis of the columns is aligned in the frame plane so that the test structure has the natural frequency characteristics similar to an actual steel frame. The beams and columns are rigidly connected by welding. The frame is fixed rigidly on a strong steel base plate.

Because of the stiff beams, the frame has effectively only three translational dofs in the horizontal direction. The damping ratio is taken to be 2% for all modes. On the basis of the mechanical properties and the member dimensions, the stiffness matrix of this 3-dof system is calculated as (N/m):

$$K_0 = 10^4 \times \begin{bmatrix} 5.07 & -5.07 & 0 \\ -5.07 & 11.07 & -6.0 \\ 0 & -6.0 & 10.04 \end{bmatrix}$$

The mass matrix of the system is found to be (kg):

$$M_0 = \begin{bmatrix} 1.81 & 0.22 & 0 \\ 0.22 & 2.48 & 0.23 \\ 0 & 0.23 & 3.01 \end{bmatrix}$$

In this experiment, the vibration was induced by a base excitation via a shake table. The excitation followed a random signal of uniform frequency spectrum in 0.1–60 Hz range, with duration of 20 s and rms $0.03 \times g$. The same excitation was repeated for three times for each test.

After the initial tests on the original test frame, the test structure was modified to represent a damaged state by replacing a third-storey column with a new element of a reduced cross-section at 32 mm × 6 mm. This resulted in a reduction of the stiffness of the third storey by approximately 18%. Table 3 summarizes the measured natural frequencies and damping ratios of the test frame before and after the "damage".

The reference 3-dof structural model can be described in a state–space form according to Eqs. (1), (8) and (10), thus

$$\mathbf{A} = \begin{bmatrix} -6.16 & -6.80 & -0.67 & 1 & 0 & 0 \\ 4.67 & -9.97 & -5.56 & 0 & 1 & 0 \\ -0.36 & -4.75 & -7.09 & 0 & 0 & 1 \\ -308 & 34000 & -3350 & 0 & 0 & 0 \\ 23300 & -49900 & 27800 & 0 & 0 & 0 \\ -17900 & 23700 & -35500 & 0 & 0 & 0 \end{bmatrix}$$

$$\mathbf{B} = \begin{bmatrix} 0.031, & -0.255, & 2.70, & 154.0, & -1270, & 13500 \end{bmatrix}$$

The failure signatures are:

$$\mathbf{P}_1 = \left[0, \quad 0, \quad 0, \quad \mathbf{M}_0^{-1} \begin{bmatrix} 1, & -1, & 0 \end{bmatrix}^{\mathrm{T}} \right]^{\mathrm{T}}$$

$$\mathbf{P}_2 = \left[0, \quad 0, \quad 0, \quad \mathbf{M}_0^{-1} \begin{bmatrix} 0, & 1, & -1 \end{bmatrix}^{\mathrm{T}} \right]^{\mathrm{T}}$$

$$\mathbf{P}_3 = \left[0, \quad 0, \quad 0, \quad \mathbf{M}_0^{-1} \begin{bmatrix} 0, & 0, & 1 \end{bmatrix}^{\mathrm{T}} \right]^{\mathrm{T}}$$

Similar to the numerical example in Section 5.1, three monitors are designed to monitor the change of stiffness in the three storeys, respectively. The measurements from the undamaged and damaged (at top storey) cases are employed to examine the effectiveness of the residual generators. Fig. 9(b) plots the residual error signals. The damage severities of individual storeys are calculated and shown in Table 4.

Table 3
Natural frequencies and damping ratios of test structure

Mode	Undamaged		K1-18% damaged	
	Frequency (Hz)	Damping (%)	Frequency (Hz)	Damping (%)
1	9.8	0. 03	9.7	0.05
2	26.7	0.04	25.6	0.04
3	41.7	0.04	40.1	0.06

Table 4
Damage severities (stiffness changes) identified before and after damage

	FE model stiffness (N/M)	No damage	K3 reduced by 18%
K3	50,700	16.4%	27.4%
K2	60,000	10.8%	10.2%
K1	40,400	−14.8%	−12.5%

It can be clearly observed from Fig. 9(b) that K_3 is significantly changed before and after the modification of the structure. On the other hand, the monitors for K_1 and K_2 exhibit insignificant changes. These results agree favorably with the actual changes induced to the test structure.

Comparing to the simulated cases presented in Section 5, the absolute "baseline" residual errors for the undamaged structure appear to be rather high as opposed to "zero" under an ideal condition. Apart from the effect of noise that inevitably exists in the measured accelerations, this is also attributable to a certain deviation of the properties used in the 3-dof structural model in representing the actual test structure. This can be confirmed by the calculated damage severity indicators shown in Table 4. In fact, the values for the undamaged state (second column in the table) may be interpreted as the extent to which the 3-dof model deviates from the actual structure. Such information could be used in a model updating procedure, which is beyond the scope of the present paper and hence will not be discussed further here. As far as the damage detection is concerned, it is the relative difference in the damage severity values between the undamaged and damaged states that really matters. In the present example, it can be deduced from the relative severity values that more than 10% reduction has occurred to the top storey (K_3).

7. Conclusions

An extended residual generator technique is presented for the time-domain damage diagnosis using acceleration response signals. The dynamic equation of a structure with acceleration responses is transformed into the standard form of EFPRG, so that the existing solution procedure of EFPRG can be applied to design the residual generators for individual components in the structure. Such residual generators are capable of detecting the occurrence and the location of damage in the structure. In addition, a damage severity indicator is incorporated to allow for an explicit calculation of the degree of damage in terms of the stiffness reduction.

Numerical examples with a swaying type of frame and a truss system demonstrate that the method can effectively determine the damage location as well as the damage severity under idealized structural and measurement conditions. The method is also applied to a laboratory experimental case with actually measured acceleration response signals. The results indicate that the accuracy of the structural model (in this case a multi-dof system) and the noise in the measurements would affect the absolute levels of the residual errors in the designed monitor; however, by examining the relative changes between the current (damaged) and a baseline (undamaged) error signals the actual structural changes can be clearly identified and assessed. In this respect, the requirement of a structural (finite element) model should not become a major issue in the implementation of the proposed approach.

It should be noted that the present method requires all degrees of freedom in the dynamic model of the structure to be measurable. Because of this, the application of the method can be problematic in the case of a continuous system such as a beam, unless the rotational measurements become available. Although the measurement of rotations is becoming increasingly affordable in some applications, it would be more desirable if the method can be extended to using other auxiliary information in lieu of the rotational measurements for the damage diagnosis. To this end, further development is required.

Appendix A. Background information for geometric technique

For a quick reference, the relevant notation, linear algebra and the preliminaries of linear dynamic systems are extracted from the literature [6,7,10] and given in this appendix. More detail information can be found from the above publications.

A.1. Space and subspace

Denote the real vector spaces by $\mathsf{X}, \mathsf{Y}, \mathsf{Z}, \ldots$, and typical elements by x, y, z, …; $d(\mathsf{X})$ is the dimension of X. A subspace S of the linear space X is presented as: $\mathsf{S} \subset \mathsf{X}$. It is a subset of X which is a linear space under the operations of vector addition and scalar multiplication inherited from X.

If $\mathsf{R}, \mathsf{S} \subset \mathsf{X}$, the internal direct sum of subspaces is written as: $\mathsf{S} \oplus \mathsf{R}$. It means the subspaces being added are known to be independent. It has $d(\mathsf{S} \oplus \mathsf{R}) = d(\mathsf{S}) + d(\mathsf{R}) - d(\mathsf{S} \cap \mathsf{R})$.

A.2. Matrix and map

If $\mathbf{B}$ is *monic*, then $\mathbf{B}^{-1}$ denotes a left inverse of $\mathbf{B}$ (i.e., $\mathbf{B}^{-1}\mathbf{B}=\mathbf{I}$). If $\mathbf{C}$ is *epic*, then $\mathbf{C}^{-r}$ denotes a left inverse of $\mathbf{C}$ (i.e., $\mathbf{C}\mathbf{C}^{-r}=\mathbf{I}$).

Let $\{x_i, i\in n\}$ be a basis for X and $\{y_j, j\in p\}$ a basis for Y. If $\mathbf{C}:\mathsf{X}\to\mathsf{Y}$ is a *map*,

$$Cx_i := c_{1i}y_1 + c_{2i}y_2 + \cdots + c_{pi}y_p, \quad i\in n$$

The symbol ":=" means equality by definition. Observe that if $x\in\mathsf{X}$ then Cx is completely determined by the Cx_i due to linearity. Matrices and linear maps are denoted by $\mathbf{A}$, $\mathbf{B}$, $\mathbf{C}$; the same symbol is used both for a matrix and its map.

Im $\mathbf{C}$ denotes the image of $\mathbf{C}$: As $\mathbf{C}:\mathsf{X}\to\mathsf{Y}$,

$$\mathrm{Im}\mathbf{C} := \{Cx : x\in\mathsf{X}\}\subset\mathsf{Y}$$

and *Ker* $\mathbf{C}$ denotes the kernel of $\mathbf{C}$:

$$Ker\mathbf{C} := \{x : x\in\mathsf{X}\&Cx=0\}\subset\mathsf{X}$$

The maps $\mathbf{A}:\mathsf{X}\to\mathsf{X}$, $\mathbf{B}:\mathsf{U}\to\mathsf{X}$, and $\mathbf{C}:\mathsf{X}\to\mathsf{Y}(d(\mathsf{X})=n, d(\mathsf{Y})=l, d(\mathsf{U})=m)$ are fixed throughout and are associated with the "*system* ($\mathbf{C}$, $\mathbf{A}$, $\mathbf{B}$)":

$$\dot{x}(t)=\mathbf{A}x(t)+\mathbf{B}u(t), \quad y(t)=\mathbf{C}x(t)$$

A.3. Factor space

Let $\mathsf{S}\subset\mathsf{X}$. Vectors $\mathbf{x},\mathbf{y}\in\mathsf{X}$ are called equivalent mod S if $x-y\in\mathsf{S}$. The *factor space* X/S is defined as the set of all equivalence classes:

$$\overline{x} := \{y; y\in\mathsf{X}, y-x\in\mathsf{S}\}, \quad x\in\mathsf{X}$$

The function $x\mapsto\overline{x}$ is a map $\mathbf{O}:\mathsf{X}\to\mathsf{X}/\mathsf{S}$, called the *canonical projection* of X on X/S. Clearly $\mathbf{O}$ is epic, and $Ker\mathbf{O}=\mathsf{S}$.

A.4. Invariant

A subspace $\mathsf{W}\subseteq\mathsf{X}$ is termed $\mathbf{A}$-*invariant* if $\mathbf{A}\mathsf{W}\subseteq\mathsf{W}$. Let $\mathsf{W}\subseteq\mathsf{X}$ be $\mathbf{A}$-*invariant*; write $\mathbf{A}:\mathsf{W}$ for the restriction of $\mathbf{A}$ to W, and $\mathbf{A}:\mathsf{X}/\mathsf{W}$ for the map induced by $\mathbf{A}$ on the factor space X/W.

If a subspace $\mathsf{W}\subseteq\mathsf{X}$ is ($\mathbf{C}$, $\mathbf{A}$)-*invariant*, there exists a map $\mathbf{D}:\mathsf{Y}\to\mathsf{X}$ such that $(\mathbf{A}+\mathbf{DC})\mathsf{W}\subseteq\mathsf{W}$. Let W be ($\mathbf{C}$, $\mathbf{A}$)-*invariant*; denote by $\underline{\mathbf{D}}(\mathsf{W})$ the class of all maps $\mathbf{D}$ such that $(\mathbf{A}+\mathbf{DC})\mathsf{W}\subseteq\mathsf{W}$. W is ($\mathbf{C}$, $\mathbf{A}$)-*invariant* if and only if $\mathbf{A}(\mathsf{W}\cap Ker\mathbf{C})\subseteq\mathsf{W}$. Let $\mathsf{L}\subseteq\mathsf{X}$; here define the family of ($\mathbf{C}$, $\mathbf{A}$)-*invariant* subspaces containing L by $\underline{\mathsf{W}}(\mathsf{L})$. Referring to Ref. [6], the family $\underline{\mathsf{W}}(\mathsf{L})$ is closed under intersection; hence $\underline{\mathsf{W}}(\mathsf{L})$contains an infimal element $\mathsf{W}^*:=\inf\underline{\mathsf{W}}(\mathsf{L})$. Also $\mathsf{W}^*=\lim\mathsf{W}^k$ where W^k is given by the following recursive algorithm [($\mathbf{C}$, $\mathbf{A}$)-***I**nvariant **S**ubspace **A**lgorithm*]:

$$\mathrm{CAISA}: \mathsf{W}^{k+1}=\mathsf{L}+\mathbf{A}(\mathsf{W}^k\cap Ker\mathbf{C}), \quad \mathsf{W}^0=0$$

A.5. Unobservablility and observability

If the subspace $\mathsf{B}=\mathrm{Im}\mathsf{B}$ and $\langle\mathsf{A}|\mathsf{B}\rangle=\mathsf{B}+\mathbf{A}\mathsf{B}+\cdots+\mathbf{A}^{n-1}\mathsf{B}$ for the infimal $\mathbf{A}$-*invariant* subspace containing B, i.e., the reachable subspace of (A,B). Write $\mathsf{K}=Ker\mathbf{C}$ and $\langle\mathsf{K}|\mathsf{A}\rangle=\mathsf{K}\cap\mathbf{A}^{-1}\mathsf{K}\cap\cdots\cap\mathbf{A}^{-1}\mathsf{K}$ for the supremal $\mathbf{A}$-*invariant* subspace contained in K, i.e., the *unobservable subspace* of ($\mathbf{C}$, $\mathbf{A}$).

A subspace $\mathsf{S}\subseteq\mathsf{X}$ is a ($\mathbf{C}$, $\mathbf{A}$) ***UnObservability Subspace*** (*u.o.s.*) if $\mathsf{S}=\langle Ker\mathbf{HC}|\mathsf{A}+\mathbf{DC}\rangle$ for some output injection map $\mathbf{D}:\mathsf{Y}\to\mathsf{X}$ and measurement mixing map $\mathbf{H}:\mathsf{Y}\to\mathsf{Y}$. Note that S is the unobservable subspace of the pair ($\mathbf{HC}$, $\mathbf{A}+\mathbf{DC}$), and the spectrum of $\mathbf{A}+\mathbf{DC}:\mathsf{X}/\mathsf{S}$ can be assigned to an arbitrary symmetric set by

appropriate choice of $\mathbf{D}$. Here use the notation $\underline{\mathsf{S}}(\mathsf{L})$ for the class of *u.o.s.* containing L. The class of *u.o.s.* $\underline{\mathsf{S}}(\mathsf{L})$ is closed under intersection; therefore, it contains an infimal element $\mathsf{S}^* := \inf \underline{\mathsf{S}}(\mathsf{L})$. Also $\mathsf{S}^* = \lim \mathsf{S}^k$ where S^k is given by the following recursive algorithm (***UnObservability Subspace Algorithm***):

$$\text{UOSA}: \mathsf{S}^{k+1} = \mathsf{W}^* + (\mathbf{A}^{-1}\mathsf{S}^k) \cap Ker\mathbf{C}, \quad \mathsf{S}^0 = \mathsf{X}$$

Moreover, $\mathsf{S}^* = \langle Ker\mathbf{C} + \mathsf{W}^* | \mathsf{A} + \mathbf{DC} \rangle$ for $\mathsf{W}^* := \inf \underline{\mathsf{W}}(\mathsf{L})$ and $\mathbf{D} \in \underline{\mathbf{D}}(\mathsf{W}^*)$. It follows that $\underline{\mathbf{D}}(\mathsf{W}^*) \subseteq \mathbf{D}(\mathsf{S}^*)$, and $Ker\mathbf{C} + \mathsf{W}^* = Ker\mathbf{C} + \mathsf{S}^*$.

A system ($\mathbf{C}$, $\mathbf{A}$, $\mathbf{B}$) is *input observable* if $\mathbf{B}$ is monic and $\mathsf{S} \cap \mathsf{B} = 0$, S is the *u.o.s.* of ($\mathbf{C}$, $\mathbf{A}$).

Appendix B. Procedure for the residual generator (monitor) design

The formulation of the EFPRG to multiple failure events is described here. A geometric approach is used to solve the EFPRG, and a procedure is described to design the residual generators for multiple failure events. More details can be found from the literature [6,7,10].

In a general EFPRG as expressed in Eq. (1), the observables are the known actuation signal $\mathbf{u}(t)$ and the output $\mathbf{y}(t)$. The maps $\mathbf{P}_i : \mathsf{M}_i \to \mathsf{X}$ is called the ith actuator failure signatures, which means $\mathbf{P}_i$ projecting the signal $m_i(t)$ to x(t). The signal $m_i(t)$ is the disturbance from the ith actuator, which is unknown. If there is no disturbance from the ith actuator, the signal $m_i(t)$ is nominally a zero signal.

The generic solvability conditions for an EFPRG problem is stated, according to Refs. [6,7], as follows: with $\mathbf{A}$, $\mathbf{C}$ and $\mathbf{P}_i$ being arbitrary matrices of dimensions $n \times n$, $l \times n$, $n \times k_i$, respectively, and let $v = \Sigma k_i$, the EFPRG generically has a solution if and only if $v \leqslant n$ and $v - \min\{k_i, i \in k\} < l$. So the $\mathbf{P}_i$ should contain as less number of columns as possible.

The most general form for a realizable residual generator for the ith actuator has been defined in Eq. (2). The following procedure is to determine the coefficients in Eq. (2) so that when the ith actuator failure mode is present, the nonzero signal $m_i(t)$ can lead to nonzero $r_i(t)$.

Generally speaking, the algorithm of this solution is that, by choosing $\mathbf{D}_0$ and $\mathbf{H}$ appropriately, one can change the observability properties of ($\mathbf{HC}$, $\mathbf{A} + \mathbf{D}_0\mathbf{C}$) in such a way that failure of all actuators are *invariant*, and the failure of all actuators are *unobservable* except the ith actuator. The first step is to keep the failures in their own subspaces; and the second step is to make the failure of the ith actuator be observed only.

The *invariant* subspace W_i^* and the *unobservable* subspace S_i^* should be defined and obtained first before solving the EFPRG.

First, the subspace W_i^* of ($\boldsymbol{C}$, $\boldsymbol{A}$)-*invariant* is given by the following CAISA [($\boldsymbol{C}$, $\boldsymbol{A}$)-***Invariant Subspace Algorithm***]:

$$\mathsf{W}_i^* = \mathsf{P}_1 \oplus \cdots \mathsf{P}_j \oplus \cdots \mathsf{P}_k \oplus \mathbf{A}\mathsf{P}_1 \oplus \cdots \mathbf{A}\mathsf{P}_j \oplus \cdots \mathbf{A}\mathsf{P}_k \quad \text{for all } P_{j \neq i}$$

With this definition, the insertion map $\mathbf{W_i} : \mathsf{W}_i^* \to \mathsf{X}$ can be written as:

$$\mathbf{W}_i = [\mathbf{P}_1, \ldots \mathbf{P}_j, \ldots \mathbf{P}_k, \mathbf{AP}_1, \ldots \mathbf{AP}_j, \ldots \mathbf{AP}_k] \quad \text{for all } P_{j \neq i}$$

Theoretically, the *unobservable* subspace S_2^* as ($\boldsymbol{C}$, $\boldsymbol{A}$)-*u.o.s.* (***UnObservability Subspace***) can be obtained theatrically by the following UOSA (***UnObservability Subspace Algorithm***):

$$\mathsf{S}_2^* + Ker\mathbf{C} = \mathsf{W}_2^* + Ker\mathbf{C}$$

In the application of FEPRG to structural dynamic system, it can be considered as $\mathsf{S}_2^* = \mathsf{W}_2^*$.

Since S_i^* has been obtained, EFPRG has a solution if and only if $\mathsf{S}_i^* \cap \mathsf{P}_i = 0$, where $\mathsf{S}_i^* := \inf \underline{\mathsf{S}}(\sum_{j \neq i} \mathsf{P}_i)$. It requires that each column of $\mathbf{W}_i$ cannot be expressed by either $c^*\mathbf{P}_i$, or $c^*\mathbf{AP_i}$ (here c is an arbitrarily constant).

The detailed steps as proposed in Ref. [7] for the design of a monitor for a specific component is summarized as follows:

- *Step* 1: Find a $\mathbf{D}$ that satisfies $\mathbf{D}_0 \in \underline{\mathbf{D}}(\mathsf{S}_2^*)$. According to UOSA, such $\mathbf{D}$ can be found by $(\mathbf{A}_c + \mathbf{DC})\mathsf{W}_2^* \subseteq \mathsf{W}_2^*$. On the basis of the suggestion by Massoumnia [7], one such $\mathbf{D}$ is given as:

$$\mathbf{D}_0 = -\mathbf{A}^2[\mathbf{P}_1, \quad \cdots \mathbf{P}_j, \quad \cdots \mathbf{P}_k](\mathbf{CA}[\mathbf{P}_1, \quad \cdots \mathbf{P}_j, \quad \cdots \mathbf{P}_k])^{-l} \quad \text{for all} \quad j \neq i$$

- *Step* 2: Find $\mathbf{O}:\mathsf{X}\to\mathsf{X}/\mathsf{S}_i^*$ as the canonical projection. Referring to the definition of the *canonical projection* in Appendix A, $\mathbf{O}$ should satisfy the following conditions: $Ker\mathbf{O}=\mathsf{S}_2^*$, which means $\mathbf{OP}_j=\mathbf{0}$ for $j\neq i$; $\mathbf{O}$ can project space X to $\mathsf{X}/\mathsf{S}_i^*$, $\mathbf{O}(\mathbf{A}+\mathbf{D}_0\mathbf{C})\mathbf{x}(t)=\mathbf{A}_0\mathbf{O}\mathbf{x}(t)$. In the application to structural dynamic system, one such $\mathbf{O}$ can be extracted from $[\mathbf{P}_1,\ \ldots,\ \mathbf{P}_k,\ \mathbf{AP}_1,\ \ldots,\ \mathbf{AP}_k]^{-1}$ by its ith row and $i+n/2$th row. At the same time $\mathbf{A}_0=\mathbf{A}+\mathbf{D}_0\mathbf{C}$: $\mathsf{X}/\mathsf{S}_i^*$ is called the map induced on the factor space $\mathsf{X}/\mathsf{S}_2^*$. In the application to structural dynamic system, $\mathbf{A}_0$ can get from $\mathbf{A}+\mathbf{D}_0\mathbf{C}$ by certain elements as:

$$\begin{bmatrix} i,i & i,i+n/2 \\ i,i+n/2 & i+n/2,i+n/2 \end{bmatrix}$$

- *Step* 3: Let $\mathbf{H}$ denote a solution of $Ker\mathbf{HC}=\mathsf{S}_i^*+Ker\mathbf{C}$, which means $\mathbf{HCP}_{j\neq i}=\mathbf{0}$. In the structural dynamic system, $\mathbf{H}$ can be calculated by

$$\mathbf{H}=\mathbf{I}-\mathbf{CA}^2\begin{bmatrix}\mathbf{P}_1, & \cdots\mathbf{P}_j, & \cdots\mathbf{P}_k\end{bmatrix}\left(\mathbf{CA}\begin{bmatrix}\mathbf{P}_1, & \cdots\mathbf{P}_j, & \cdots\mathbf{P}_k\end{bmatrix}\right)^{-l}\quad \text{for all } j\neq i$$

- *Step* 4: Let $\mathbf{M}$ be the unique solution of $\mathbf{MO}=\mathbf{HC}$.
- *Step* 5: Let $\mathbf{F}=\mathbf{A}_0+\mathbf{D}_1\mathbf{M}$ and $\mathrm{eig}(\mathbf{F})=\Lambda$. Λ is an arbitrary self-conjugate set with negative eigenvalues. Hence $\mathbf{D}_1$ is also found. In the example of structural dynamic example, a suggestion is to taking $\Lambda=[-1,0;\ 0,-1]$ first, then $\mathbf{F}=\mathbf{A}_0+\mathbf{D}_1\mathbf{M}$ can be found according to $\mathbf{A}_0$ and $\mathbf{M}$. Hence $\mathbf{D}_1$ also can be found.
- *Step* 6: With $\mathbf{O}^{-\mathrm{r}}$ denoting a right inverse of $\mathbf{O}$, calculate $\mathrm{D}=\mathbf{D}_0+\mathbf{O}^{-\mathrm{r}}\mathbf{D}_1\mathbf{H}$, $\mathbf{E}=\mathbf{OD}$, $\mathbf{G}=\mathbf{OB}$.

Following these steps the coefficients [F, E, G, M, H] has been calculated, which satisfies the requirement of the solution as an indicator of the ith actuator.

Appendix C. Discussion on the decomposition of stiffness matrix

As noted in Section 3, in order to satisfy the generic solvability conditions for EFPRG (refer to Appendix), the failure signatures $\mathbf{P}_i$ should contain as less number of columns as possible. This necessitates a proper decomposition of the damage effect of the model parameters.

The stiffness matrix of an element can be decomposed into the product of matrices with fewer columns and fewer rows, respectively, than the original stiffness matrix. For example:

The stiffness matrix of a spring element:

$$\mathbf{k}=k_0\begin{bmatrix}1 & -1\\ -1 & 1\end{bmatrix}=k_0\begin{bmatrix}-1\\ 1\end{bmatrix}\begin{bmatrix}-1 & 1\end{bmatrix}$$

Thus, $\mathbf{p}_i=\begin{bmatrix}-1 & 1\end{bmatrix}^{\mathrm{T}}, \mathbf{q}_i=\begin{bmatrix}-1 & 1\end{bmatrix}$.

The stiffness matrix of a truss element (with s and c denoting the directional sine and cosine, respectively):

$$\mathbf{k}=\frac{EA}{l}\begin{bmatrix}c^2 & cs & -c^2 & -cs\\ cs & s^2 & -cs & -s^2\\ -c^2 & -cs & c^2 & cs\\ -cs & -s^2 & cs & s^2\end{bmatrix}=\frac{EA}{l}\begin{bmatrix}c\\ s\\ -c\\ -s\end{bmatrix}\begin{bmatrix}c & s & -c & -s\end{bmatrix}$$

The stiffness matrix of a beam element:

$$\mathbf{k}=\frac{EI}{l^3}\begin{bmatrix}12 & 6l & -12 & 6l\\ 6l & 4l^2 & -6l & 2l^2\\ -12 & -6l & 12 & -6l\\ 6l & 2l^2 & -6l & 4l^2\end{bmatrix}=\frac{2EI}{l^3}\begin{bmatrix}1 & 1\\ l & 0\\ -1 & -1\\ 0 & l\end{bmatrix}\begin{bmatrix}3 & 2l & -3 & l\\ 3 & l & -3 & 2l\end{bmatrix}$$

In the assembled global stiffness matrix, the contribution of each member matrix can be looked on as the member stiffness matrix entries inserting into a null matrix with the dimension of the global stiffness matrix. So the contribution of the ith member in the global stiffness matrix, denoted as $\mathbf{K}_{0i}$, also can be decomposed in the same way. Consequently, $\Delta\mathbf{K}$ can be written in the following form for all possible damage in these members:

$$\Delta\mathbf{K} = \mathbf{M}_0^{-1} \sum_{i=1}^{k} \alpha_i \mathbf{K}_{0i} = \sum_{i=1}^{k} \mathbf{p}_i \mathbf{q}_i \alpha_i$$

where k is the number of members that may be subject to damage, α_i denotes the damage severity of the ith member; if no damage occurs, $\alpha_i = 0$.

This leads to the establishment of Eq. (10) in Section 4.

References

[1] S.F. Masri, M. Nakamura, A.G. Chassiakos, T.K. Caughey, Neural network approach to detection of changes in structural parameters, *Journal of Engineering Mechanics ASCE* 122 (4) (1996) 350–360.

[2] H. Sohn, C.R. Farrar, Damage diagnosis using time series analysis of vibration signals, *Smart Materials and Structures* 10 (2001) 1–6.

[3] Y. Lu, F. Gao, A novel time-domain auto-regressive model for structural damage diagnosis, *Journal of Sound and Vibration* 283 (3–5) (2005) 1031–1049.

[4] F. Gao, Y. Lu, A Kalman-filter based time-domain analysis for structural damage diagnosis with noisy signals, *Journal of Sound and Vibration* 297 (3–5) (2006) 916–930.

[5] T. W. Ma, H. T. Yang, C. C. Chang, Structural health monitoring using time-domain residual generator technique, *Proceedings of the Fourth International Workshop on Structural Health Monitoring: Structural Health Monitoring 2003*, Stanford University, pp. 445–452.

[6] M.A. Massoumnia, A geometric approach to the synthesis of failure detection filters, *IEEE Transactions of Automatic Control* AC-31 (1986) 839–846.

[7] M.A. Massoumnia, G.C. Verghese, A.S. Willsky, Failure detection and identification, *IEEE Transactions of Automatic Control* AC-34 (1989) 316–321.

[8] T.W. Ma, H.T. Yang, C.-C. Chang, Structural damage diagnosis and assessment under seismic excitations, *Journal of Engineering Mechanics ASCE* 131 (10) (2005) 1036–1045.

[9] C.-G. Lee, C.-B. Yun, Parameter identification of linear structural dynamic systems, *Computer & Structures* 40 (6) (1991) 1475–1487.

[10] W.M. Wonham, *Linear Multivariable Control: A Geometric Approach*, Springer, New York, 1985.

[11] C.L. Phillips, H.T. Nagle, *Digital Control System Analysis and Design*, Prentice-Hall, Englewood Cliffs, NJ, 1984.